Eur. Phys. J. E **3**, 63–70 (2000)

THE EUROPEAN PHYSICAL JOURNAL E

EDP Sciences

Thermodynamics and X-ray studies of 2-alcohol monolayers: Two-dimensional phase diagrams

C. Alonso[1], F. Artzner[2], J. Lajzerowicz[1], G. Grubel[3], N. Boudet[3], F. Rieutord[3], J.M. Petit[3], and A. Renault[1a]

[1] Laboratoire de Spectrométrie Physique, UMR C5588, Université Joseph Fourier-CNRS, BP 87, 38402 Saint Martin d'Hères Cedex, France
[2] Laboratoire de Physico-Chimie des Systèmes Polyphasés, UMR 8612, CNRS-Université Paris Sud, 5 rue J.B. Clément, 92296 Chatenay-Malabry Cedex, France
[3] ESRF, BP220, F-38043 Grenoble Cedex, France

Received 13 October 1999 and Received in final form 20 March 2000

Abstract. Monolayers of short chiral alcohols at the water surface provide a simple model for chiral interactions between molecules. This paper is focused on alcohols with two particular chain lengths, 2-tridecanol (2C13) and 2-tetradecanol (2C14). Thermodynamic and structural parameters were measured, varying the ratio of left and right enantiomers within monolayers. The evolution of melting temperatures and entropies is not consistent with the formation of a racemate. Grazing X-ray diffraction, revealing the molecular stacking, shows clearly that there is no chiral separation. In these two compounds molecules spontaneously self-assemble at the water surface as a solid solution. The chiral polar head-group is partially screened by the chain thermal disorder of the rotator phase. 2-tridecanol exhibits a hexagonal rotator phase stable in time and independent of temperature. Experiments performed close to the melting point show pre-transitional effects for mixtures different from 50/50. This broadening of the peak can be related to defects in 2D crystals, phenomena already observed for the melting of some 3D systems.

PACS. 61.10.-i X-ray diffraction and scattering – 64.70.Dv Solid-liquid transitions – 82.65.Dp Thermodynamics of surfaces and interfaces

1 Introduction

Most natural molecules are chiral and nature, contrary to the chemist, can perfectly select either enantiomer. The understanding of 3D interactions between chiral molecules is of great importance for many scientific fields [1], in particular for pharmacology where consequences can be tragic [2,3]. As most of the receptors in the human body are chiral, the absolute conformation of molecules is crucial, one enantiomer can have a therapeutic action while the other have no action, the latter can even be poisonous. Enantiomers of the same compound often possess very different properties. Another example is the dipeptide Aspartame which is classically used as a sugar substitute, its natural form SS tastes sweet while the artificial RR seems bitter. In order to enhance molecular interactions, Arnett proposed to investigate molecules confined on a surface [4]. The surface potential forces molecules to be nearly vertical, with the chiral part of molecules next to one another, thus chiral interactions should probably be enhanced. Previous studies show different behaviors for binary mixtures of enantiomers confined in a two-dimensional space [5–9] dependent on the interaction between neighboring molecules and between molecules and the subphase (covalent, electrostatic, hydrogen bonds). In some cases homo or heterochiral behavior can be predicted according to theory [10] but the model is limited to very simple molecules self-assembled in Langmuir films. Recently the effects of chirality in Langmuir monolayers have been studied in order to obtain some indications about biological mechanisms [5] which involves complex molecules and thus different possible ways of interactions.

In order to extract information on chiral interactions we employed very short and simple molecules (2-alcohols with 13 and 14 carbons). There are two main interactions between these molecules: hydrophobic, which controls the stacking, and chiral, which should impose the symmetry. Monolayers of short 1-alcohols have been well described in recent years [11,12]. We can compare our results with non-chiral molecules with the same chemical formulae and try to deduce the role of the chiral center.

Results for racemic mixtures of 2-alcohols were previously presented, the two main points are the following [13]. First, the liquid-solid transition of monolayers is clearly first order for all chain lengths between 10 and

[a] *Present address*: Groupe Matière Condensée et Matériaux, Université Rennes 1, Campus de Beaulieu - Bât. 11A, 35042 Rennes Cedex, France.
e-mail: `anne.renault@univ-rennes1.fr`

17 carbons but becomes less so as the number of carbons decreases. Second, the solid state is characterized by a hexagonal structure, stable in time for odd alcohols but not for even ones. In this paper we present results for two different chain lengths (13 and 14 carbons). We highlight the influence of the chiral center on the bidimensional organization. In this way monolayers of racemic mixtures, of pure enantiomers and of different mixtures of both enantiomers were studied. Phase diagrams (melting temperature *vs.* proportion of enantiomers) were established and completed with a structural study, in order to connect thermodynamical parameters to molecular stacking. And in addition, the comparison between the two compounds can give some indications about the odd/even effect previously detected.

The first part of this paper contains a description of experimental techniques including ellipsometry, surface tension measurements and grazing incidence X-ray diffraction. The second part is devoted to experimental results for 2-tridecanol on the one hand and 2-tetradecanol on the other. For each one, thermodynamic and structural results and their analysis are exposed.

2 Experimental techniques

Racemic of 2-tridecanol ((±)2C13) and 2-tetradecanol ((±)2C14) were used as received from Aldrich SA (purity > 99%). Pure enantiomers ((S)C13 and (S)C14) were synthesized by copper-catalyzed Grignard methyl oxirane opening [14] (purity > 99%). Mixtures of enantiomers are noted (75(S)/25(R))2C13 for example with the numerical prefix indicating the percentage of left and right molecules in the mixture. The subphase is always ultrapure water with a conductivity of $18\,\mathrm{M}\Omega\,\mathrm{cm}^{-1}$.

The size of the molecules obliged us to develop a new method of monolayer deposition because the standard way of generating a phase transition in Langmuir films with movable barriers is not applicable for water soluble molecules [15]. A drop of pure alcohol is deposited on the water surface, a monolayer spreads spontaneously and remains in equilibrium with the reservoir drop. Any loss of matter at the surface by evaporation or dissolution is compensated by the reservoir (see Fig. 1). Phase transitions are induced by temperature variations.

Ellipsometry and surface tension were used to measure transition temperature and entropies on the same set-up in the same time. Surface tension is measured by a platinum Wilhemy plate, weighed by a SARTORIUS balance which yields a stability of 0.5 mN/m over 12 hours. For ellipsometry, the incident beam is produced by a He-Ne laser followed by a GLAN-THOMPSON polariser. The reflected beam is analyzed by a $\lambda/4$ wave plate and a GLAN-THOMPSON analyzer. It is then collected in a photomultiplier. The angle of incidence is 1.00 degree away from the Brewster angle. The zero intensity is continuously monitored by means of small variations of the computer-controlled polarizer and analyzer. In this configuration, the analyzer rotation angle is half the phase difference δ between the two orthogonal polarizations [16]. The trough

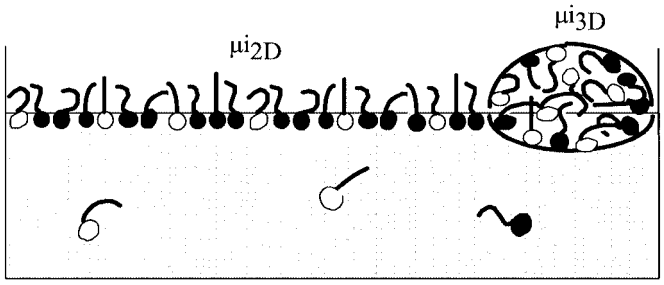

Fig. 1. Schematic representation of the experimental system, a monolayer in equilibrium with a reservoir drop. μ is the chemical potential for monolayer (2D) or drop (3D) and for each kind of molecules (i = R or S). Black and white polar head distinguish, respectively, right and left enantiomers.

used is made of Teflon (depth: 8 mm) and inserted in a closed metallic container. The temperature, regulated by circulating water, is measured by a Pt resistance in a stainless steel rod dipped into the trough. The thermal stability is about 0.05 K/hour. All measurements were performed with temperature varied at a rate speed of 10 °C/hour.

Grazing incidence X-ray diffraction (GIXD) experiments were carried out at ESRF (European Synchrotron Radiation Facility) in Grenoble, on two beamlines. The BM32 beamline is located on a bending magnet. A double diamond monochromator selects a single radiation of wavelength $\lambda = 1.38$ Å. The beam is focused on the sample by the second diamond crystal. A mirror deflects this beam onto the sample with an incident angle $\alpha = 2\,\mathrm{mrad} = 0.85\alpha_c$ ($\alpha_c = 2.3$ mrad critical angle for a water subphase at the energy of 9 keV). Before the sample, X-rays are monitored by a NaI scintillator. The diffracted beam is analyzed by Soller slits (resolution of $4 \cdot 10^{-3}$ Å^{-1}) and then collected in a PSD (Position Sensitive Detector). The second beamline used, ID10A is an ondulator beamline on wich a Si(111) monochromator in asymmetric Laue geometry is used to produce a monochromatic X-ray beam of wavelength $\lambda = 1.41$ Å. A Ge(111) crystal in position of Bragg reflection is used to analyze the diffracted beam and reach an angular resolution of $5 \cdot 10^{-3}$ deg. corresponding to $4 \cdot 10^{-4}$ Å^{-1} [17].

A special circular Teflon trough of diameter 80 mm has been designed for X-ray diffraction experiments. It can continuously rotate around a vertical axis at the speed of 1 rd/mn, in order to average the crystalline powder structure. The temperature within the trough is regulated by circulation of a thermal liquid (range of temperature [250 K–330 K]). In order to reduce capillary waves at the water-air interface, a flat silicon block is immersed in the trough, leaving a typical thickness of 300 μm of water under the alcohol monolayer. In order to preserve the sample height during long experiments, a water level regulation system which leads to a stability of ±5 μm over several hours was developed [18].

3 Experimental results

3.1 2-tridecanol

There is not much information on the 3D packing of 2-alcohols due to the lack of enantiomers. As the synthesis of (S)C13 was performed, the first step of this study was to establish the melting temperature as a function of the ratio of enantiomers diagram to determine the type of stacking. Spectra recorded by DSC (Differential Scanning Calorimetry) for concentrations between 60% and 90% of (S)C13 show two peaks, one of them is common to all spectra and can be attributed to the eutectic concentration, while the other one gives the melting temperature of the complement. Thus the phase diagram is typical of a racemate with ranges of solid solution like even ones [13] and like the major part of crystals of chiral molecules: more than 90% of studied crystals are racemate [1].

Data for the two-dimensional phase diagram are reported in Table 1. The monolayer melting is indicated by a jump of the ellipsometric angle and a break of slope of the surface tension curves. The melting entropy is calculated from the slopes of surface tension *vs.* temperature curves. The area per molecule in the liquid phase can also be calculated from the melting entropy and the area per molecule in the solid phase [19] (21.5 Å^2 according to GIXD measurements). Figure 2a) shows that all melting temperatures are more or less equal. Moreover, all monolayers have the same entropy variations.

Whatever the ratio of both enantiomers, all monolayers GIXD patterns exhibit one single narrow Bragg peak. This is typical of a hexagonal rotator phase. Figure 3 shows the diffraction peaks for (±)2C13 and (S)2C13 recorded at the same temperature. The maxima are not at the same position and the comparison of peak positions for different mixtures of both enantiomers shows that lattice parameters are all different (see Fig. 4). This means that there is no chiral separation in this system. But to reach this conclusion, a high resolution set-up is necessary as the difference of lattice parameters is very small and can only be detected with a crystal analyzer. This also allows the measurements of Bragg peak widths and to analyze the shape of Bragg peaks. It is known that for 2D systems, the structure factor follows the law [20]

$$S(Q) \cong |Q - Q_0|^{-(2-\eta)}. \quad (1)$$

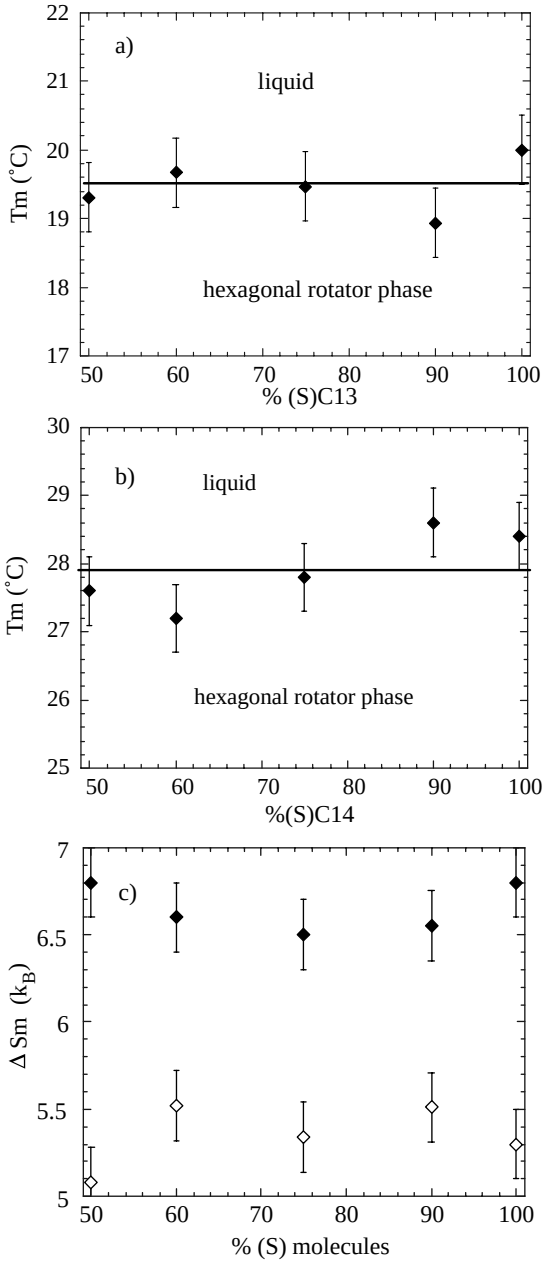

Fig. 2. Thermodynamic phase diagram: a) melting temperature *vs.* ratio of enantiomers for 2-tridecanol, b) 2-tetradecanol, c) melting entropies for 2-tetradecanol (♦) and 2-tridecanol (◊).

In two dimensions there is no long-range order due to thermal fluctuations and as a consequence diffraction peaks exhibit a power law shape. The high resolution of the ID10A set-up allows the determination of η with a good accuracy from line shape analysis and thus to quantify some pre-transitional effects [18], using a fitting program developed in our laboratory. For (±)2C13, the Bragg peak disappears suddenly at the transition without any evolution before, thus the liquid-solid transition is clearly first order. For mixtures other than 50/50 a temperature evolution of the Bragg peak is observed. For example, the diffraction peaks recorded for several temperatures for a monolayer of (60(S)/40(R))2C13 are reported in Figure 5. One can see that the intensity decreases regularly a few degrees below the melting point with a broadening of the peak. This evolution can be quantified. In Figure 6, the power law parameter η (proportional to the inverse of rigidity) for a monolayer of (75(S)/25(R))2C13 is reported. Close to melting, η increases quickly indicating a decreasing of the monolayer rigidity. The addition of (S)2C13 to the racemic mixture induces clear pre-transitional effects. All results presented were obtained with a liquid reservoir drop but as the hexagonal phase re-

Table 1. Temperature, surface tension, area per molecule and entropy characterizing the melting of monolayers of 2-tridecanol. The first column is the fraction of (S)2C13 within the sample.

%(S)2C13	$T_{\rm m} \pm 1(\,^\circ\mathrm{C})$	$\gamma_{\rm m} \pm 1(\,\mathrm{mN/m})$	$a_{\rm L} \pm 1(\mathrm{\AA}^2)$	$\Delta S_{\rm m} \pm 0.2(k_{\rm B})$
50	19.3	31.2	26.8	5.1
60	19.7	31.0	27.2	5.5
75	19.5	30.2	27.0	5.3
90	18.9	31.6	27.2	5.5
100	20.0	31.7	27.0	5.3

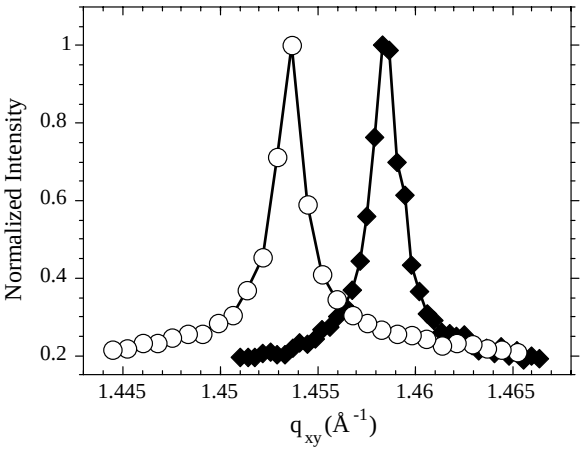

Fig. 3. Comparison between Bragg peaks for monolayers of 2C13 at the same temperature (19.1 °C), pure enantiomer (◯) and racemic mixture (⧫).

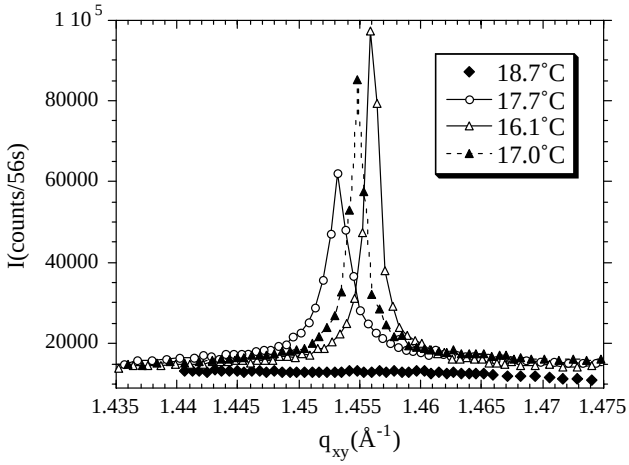

Fig. 5. Bragg peak evolution with temperature for a monolayer of (60(S)/40(R))2C13.

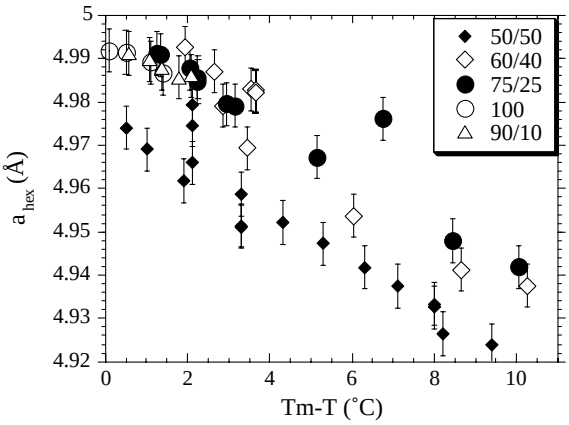

Fig. 4. Evolution of lattice parameters ($a_{\rm hex}$) *vs.* melting temperature ($T_{\rm m}$)-sample temperature (T) for several mixtures of (R) and (S)2C13.

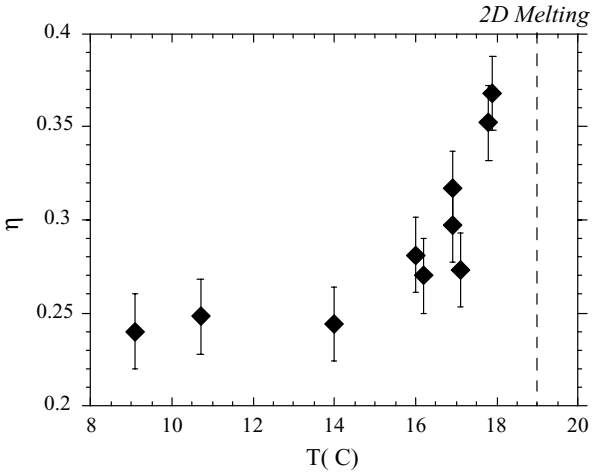

Fig. 6. Evolution as a function of temperature of η parameter for a monolayer of (75(S)/25(R))2C13.

mains stable we have done the same with a solid reservoir. The drop crystallization slows down or even stops diffusion of molecules between 2D and 3D phases which does not modify the microscopic structural properties such as rigidity (η) and lattice parameter, but affects the quality and the size of the crystal as revealed by the decrease of the coherence length. For a monolayer of pure (S)2C13, we are limited upon cooling because of the drop crystallization ($T_{\rm c3D} = 12.5\,^\circ\mathrm{C}$), but the points recorded do not show any evolution of the diffraction peak close to melting.

3.2 2-tetradecanol

Thermodynamical results characterizing the 2D liquid-solid transition for several mixtures of (R) and (S)2C14

Table 2. Temperature, surface tension, area per molecule and entropy characterizing the melting of monolayers of 2-tetradecanol. The first column is the fraction of (S)2C14 within the sample.

%(S)2C14	$T_m \pm 1(^\circ C)$	$\gamma_m \pm 1(mN/m)$	$a_L \pm 1(Å^2)$	$\Delta S_m \pm 0.2(k_B)$
50	27.6	33.1	28.4	6.8
60	27.2	31.2	28.4	6.6
75	27.8	32.1	28.3	6.5
90	28.6	30.9	28.4	6.5
100	28.4	32.5	28.5	6.8

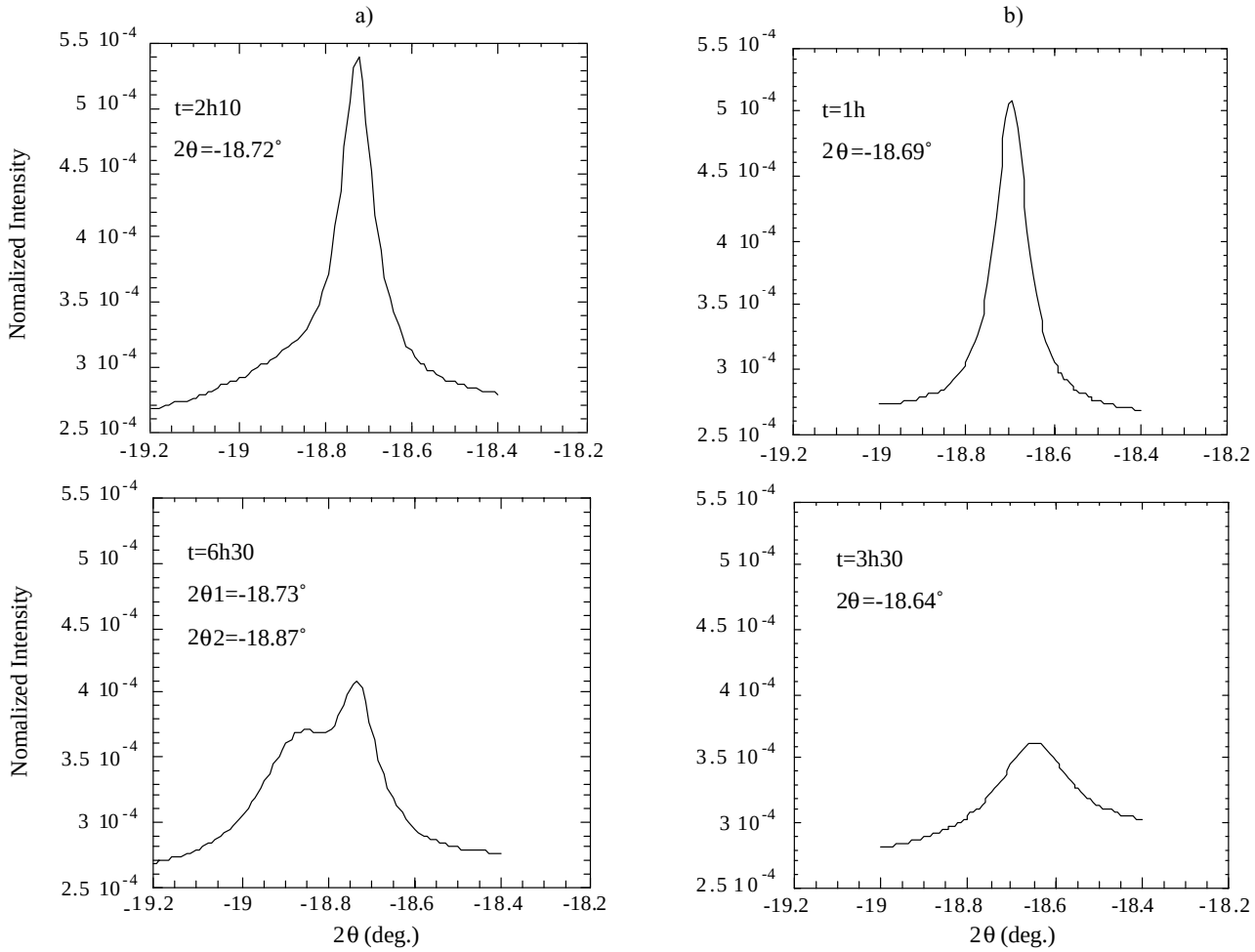

Fig. 7. Evolution with time of the Bragg peak for monolayers of 2-tetradecanol: a) racemic mixture and b) pure enantiomer at 23.1 °C.

enantiomers are reported in Table 2. All these results have been obtained during temperature cycles avoiding the crystallization of the reservoir drop. Temperature and melting entropy depend only weakly on the (S)2C14 concentration as in 2-tridecanol (Fig. 2b) and 2c)). The average difference between the melting entropies of the two compounds, 2-tetradecanol and 2-tridecanol is $1k_B$ which corresponds to the entropy of one more methylene.

GIXD experiments were carried out on the BM32 beamline because diffraction peaks are broader than for 2-tridecanol and the high resolution is not suitable. Figure 7 summarizes the results. A racemic mixture ((±)2C14) and pure enantiomer ((S)2C14) monolayers were deposited in their liquid phase. The temperature was then decreased to 23.1 °C which is between the 2D melting point (28.5 °C) and the 3D one (20 °C) to try to avoid any effect of drop crystallization. At the beginning we observe one single peak for both, typical of a hexagonal phase with molecules perpendicular to the interface. It is important to notice that the crystalline phases are the same for the two compounds, but the lattice parameter is smaller for the racemic mixture.

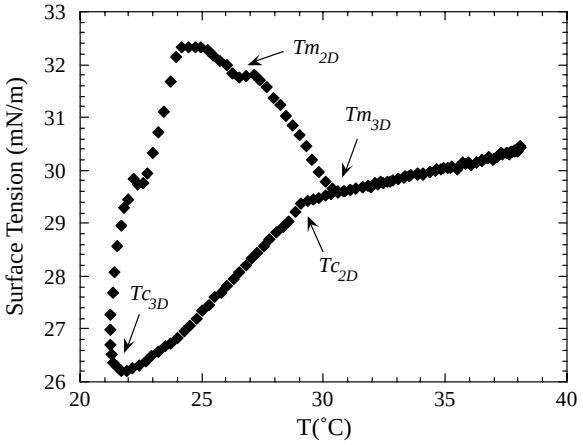

Fig. 8. Variations of surface tension *vs.* temperature for a monolayer of (±)2C14. Melting (T_m) and crystallization temperatures (T_c) of the drop (3D) and the monolayer (2D) are reported.

- For the (±)2C14, we observe a shift of the peak with a splitting. It can be seen (Fig. 7a)) that after 6.5 hours there is no evolution any more and the diffraction pattern corresponds to a centered rectangular lattice with two molecules per unit cell. This comes from a distortion of the 60 ° angle by 1 °. The loss of hexagonal symmetry is usually due to a tilt of molecules but the Bragg rods show that molecules remain perpendicular to the interface. In this particular case the splitting may be due to the fact that the lattice unit cell contains two non-equivalent molecules. One can imagine that at that time molecules no longer freely rotate around their long axis, the distinction between (R) and (S) molecules is then possible and the formation of a racemate could be expected.
- For (S)2C14 monolayer (Fig. 7b)), the intensity of the Bragg peak decreases and after 3.5 hours the monolayer is not crystalline any more. Bragg rods do not show any change in the orientation of molecules during this evolution. Nevertheless, the ellipsometric response is the same as in the crystalline phase, the density of both phases are very close to each other.

For the two compounds, surface tension measurements recorded in the same conditions show that the reservoir drops could have crystallized during these experiments. These phenomena could be induced by the variation of surface pressure consecutive to the drop crystallization (see Fig. 8) and are not necessarily pure 2D ones. However the immediate conclusion is that as for 2C13, there is no chiral separation.

4 Discussion

4.1 Relation between 2D and 3D enantiomeric excesses

First of all, for a correct interpretation of phase diagrams, it is necessary to know the enantiomeric excess in the monolayer. Our particular experimental system allows the diffusion of molecules from the drop to the monolayer due to the different chemical potentials as is indicated in Figure 1, but also *vice versa.* One can imagine that the surface could have favored only one particular concentration, 50/50 for heterochiral behavior and 100/0 for homochiral one. A theoretical model was developed to estimate the surface enantiomeric excess. This simple statistical model only considers the chiral interactions between first neighbors but it is enough to link the enantiomeric excesses of drop and monolayer [21].

The equilibrium between drop and monolayer is described by the equality of chemical potentials which can be calculated using the Bragg-William method [22]. U_{RR}, U_{SS} and U_{RS} are the short range interaction energies for homo and heterochiral pairs. The subscripts S and R correspond to left- and right-handed molecules. There is chiral discrimination if $U_{RR} = U_{SS} \neq U_{RS}$ and the condition for chiral separation is $U_{RR} < U_{RS}$. Other parameters are z, the number of nearest neighbors, N_S and N_R the numbers of S and R molecules and $N = N_R + N_S$ the total number of molecules.

- The expression for the energy U is in the Bragg William approximation:

$$U = zN_S\left[\left(\frac{N_S}{N}\right)U_{SS} + \left(\frac{N_R}{N}\right)U_{SR}\right] + zN_R\left[\left(\frac{N_R}{N}\right)U_{RR} + \left(\frac{N_S}{N}\right)U_{SR}\right], \quad (2)$$

$$U = \frac{z}{2N}\left[(N_S + N_R)^2(U_{SR} + U_{RR}) - (N_R - N_S)^2(U_{SR} - U_{RR})\right]. \quad (3)$$

- The exact form of the entropy S is

$$S = k_B \ln\left[\frac{(N_S + N_R)}{N_R!N_S!}\right]. \quad (4)$$

By application of the Stirling formulae and in the limit $(N_R - N_S)/N \ll 1$, for the second order:

$$S = k_B(N_S + N_R)\left[\ln 2 - \frac{1}{2}\frac{(N_R - N_S)^2}{(N_R + N_S)^2}\right]. \quad (5)$$

Terms of odd exponent are deleted by symmetry: S has to be invariant by the exchange of R and S molecules because the number of conformations does not depend on the chirality of one single molecule.

- The chemical potential is given by $\mu_i = (\partial G/\partial N_i)_{T,P}$ i = R or S with $G = U - TS$ in this particular case because U depends on pressure:

$$\begin{cases} \mu_{\mathrm{R}} = [z(U_{\mathrm{RR}} + U_{\mathrm{SR}}) - k_{\mathrm{B}}T\ln 2] \\ \qquad + \dfrac{1}{2}[k_{\mathrm{B}}T - z(U_{\mathrm{SR}} - U_{\mathrm{RR}})] \\ \qquad \times \left[2\dfrac{(N_{\mathrm{R}} - N_{\mathrm{S}})}{(N_{\mathrm{R}} + N_{\mathrm{S}})} - \left(\dfrac{N_{\mathrm{R}} - N_{\mathrm{S}}}{N_{\mathrm{R}} + N_{\mathrm{S}}}\right)^2 \right], \\ \mu_{\mathrm{S}} = [z(U_{\mathrm{RR}} + U_{\mathrm{SR}}) - k_{\mathrm{B}}T\ln 2] \\ \qquad + \dfrac{1}{2}[k_{\mathrm{B}}T - z(U_{\mathrm{SR}} - U_{\mathrm{RR}})] \\ \qquad \times \left[-2\dfrac{(N_{\mathrm{R}} - N_{\mathrm{S}})}{(N_{\mathrm{R}} + N_{\mathrm{S}})} - \left(\dfrac{N_{\mathrm{R}} - N_{\mathrm{S}}}{N_{\mathrm{R}} + N_{\mathrm{S}}}\right)^2 \right]. \end{cases} \tag{6}$$

Concentrations of S and R molecules are $\chi_{\mathrm{R}} = N_{\mathrm{R}}/(N_{\mathrm{R}} + N_{\mathrm{S}})$ and $\chi_{\mathrm{S}} = N_{\mathrm{S}}/(N_{\mathrm{R}} + N_{\mathrm{S}})$ but the pertinent parameter in our system is the enantiomeric excess

$$\chi = \chi_{\mathrm{S}} - \chi_{\mathrm{R}}. \tag{7}$$

Addition and difference of homo and heterochiral interaction energies are also more representative than the absolute energies:

$$\begin{cases} U_1 = z(U_{\mathrm{SR}} + U_{\mathrm{RR}}), \\ U_2 = z(U_{\mathrm{SR}} + U_{\mathrm{RR}}). \end{cases} \tag{8}$$

Thus, the first order for χ is

$$\begin{cases} \mu_{\mathrm{R}} = (U_1 - k_{\mathrm{B}}T\ln 2) - (k_{\mathrm{B}}T - U_2)\chi, \\ \mu_{\mathrm{S}} = (U_1 - k_{\mathrm{B}}T\ln 2) + (k_{\mathrm{B}}T - U_2)\chi. \end{cases} \tag{9}$$

These equations are valid for molecules in a 3D environment as well as molecules in a 2D one. As equilibrium conditions between drop and monolayer are

$$\mu_{\mathrm{R}}^{\mathrm{2D}} = \mu_{\mathrm{R}}^{\mathrm{3D}}, \tag{10a}$$

$$\mu_{\mathrm{S}}^{\mathrm{2D}} = \mu_{\mathrm{S}}^{\mathrm{3D}}. \tag{10b}$$

One can immediately write

$$\begin{aligned} \left(k_{\mathrm{B}}T - U_2^{\mathrm{2D}}\right)\chi^{\mathrm{2D}} - \left(k_{\mathrm{B}}T - U_2^{\mathrm{3D}}\right)\chi^{\mathrm{3D}} \\ = \left(U_1^{\mathrm{2D}} - k_{\mathrm{B}}T\ln 2\right) - \left(U_1^{\mathrm{3D}} - k_{\mathrm{B}}T\ln 2\right), \end{aligned} \tag{11}$$

the superscripts 2D and 3D respectively refer to the monolayer and the drop. This expression has to match with the high temperature limit when the drop is a racemic mixture ($\chi^{\mathrm{3D}} = 0$), which necessarily implies $\chi^{\mathrm{2D}} = 0$. Finally:

$$\chi^{\mathrm{2D}} = \left(\frac{k_{\mathrm{B}}T - U_2^{\mathrm{3D}}}{k_{\mathrm{B}}T - U_2^{\mathrm{2D}}}\right)\chi^{\mathrm{3D}}. \tag{12}$$

The excess in the bidimensional phase is determined by relative values of thermal energy and chiral discrimination. For high temperatures, effects due to chiral discrimination are negligible. Otherwise, as chiral interactions are not the same in 2 or 3 dimensions, the enantiomeric excesses are not necessarily equal. It is a consequence of the 2D/3D equilibrium which does not result from the concentrations equilibrium but from the pressure. The physical phenomenon allowing pressure changes is the variation of the density within the monolayer.

U_2 can be evaluated by semi-empirical methods. It was previously found that the ratio U_2/U_1 is close to 10^{-2} [23], however this is not necessary for our interpretation. Diffraction experiments prove that all mixtures are different because all lattice parameters are different. The surface accepts enantiomeric excess and does not impose one single concentration.

4.2 Interpretation of phase diagrams

The three possible kinds of crystals are racemate, conglomerate or solid solution. Or, in other words, ordered crystal, separation of right and left crystals and disordered crystal [1]. The variations of melting temperature with the ratio of enantiomers in 3D systems allow to determine the kind of stacking. The same thing can be done for 2D systems but an additional parameter can also give information, the melting entropy. As was previously said, we can deduce ΔS_{2D} from the measurements of surface tension variations *vs.* temperature [13,19]. Total entropy of a binary mixture contains an entropy mixing term equal to $k_{\mathrm{B}}(x_{\mathrm{R}}\ln x_{\mathrm{R}} + x_{\mathrm{S}}\ln x_{\mathrm{S}})$ where k_{B} is the Boltzmann constant and x_{I} is the molar fraction of the I-type molecule. Thus the difference ΔS_{2D} between the liquid and the solid state would be the same for a disordered crystal as for pure enantiomers, for which no entropy mixture term has to be considered, whereas the ΔS_{2D} of an ordered mixture (racemate or conglomerate) would be higher. For the 2-alcohols, the entropies for racemic mixture and the corresponding enantiomer are equal which means that the mixture is a solid solution.

This conclusion is reinforced by GIXD results. For the two chain length, racemic mixture and pure enantiomer monolayers present the same crystalline phases but with distinct lattice parameters. This prevents the possibility of a conglomerate. Moreover, a racemate lattice requires at least 2 molecules per unit cell (one R, one S). The observed hexagonal lattice, which has only one molecule per unit cell, contradicts the possibility of a racemate formation and rotational disorder seems more probable in a solid solution. The smaller lattice spacing observed for racemic mixtures than for pure enantiomers indicates an attractive interaction between right and left molecules but not strong enough to stabilize the formation of a racemate compound. This has already been observed for some binary mixtures of lipids [24] for example. The small size of the aliphatic chains allows rotational disorder even at a temperature far from melting. In that way, left and right molecules become equivalent and the chiral effects are cancelled.

4.3 Softening of monolayers

Free rotation of molecules frustrates the chirality effect, but the evolution of the phase up to the melting of the

monolayer depends on the ratio of enantiomers. Monolayers of (±)2C13 and (S)2C13 do not present any pre-transitional effects whereas in other mixtures, monolayers become softer close to the melting point. The absence of any pre-transitional effects for racemic and pure enantiomer monolayers is consistent with surface tension measurements which show that the solid/liquid transition is first order. Calculations predict it to be continuous only for less than 9 carbons in the chain. However, previous results obtained for monolayers of 1-alcohols showed that ellipsometry is not sensitive enough to detect weak pre-transitional effects, whereas the diffraction with a high resolution set-up allows to detect and quantify these effects. For short chain 1-alcohols (less than 10 carbons), this kind of behavior is commonly interpreted as the melting of a hexatic phase [18]. This is not relevant for 2-alcohol where the presence or absence of pre-transitional effects depends on the concentration of left-handed molecules in the drop and not on the chain length (similar variation has been observed for 2C17 [21]). Thus, it can not only be due to the well-known effect of melting of a hexatic phase [20]. It has to be induced by the mixture of both enantiomers. The addition of left-handed molecules to the racemic mixture can be considered as adding impurities which disturb the perfect periodicity of the crystal. As in three dimensions it can be interpreted in terms of thermal motion of grain boundaries. The result is the decreasing of the monolayer rigidity.

5 Conclusion

The study of chiral molecules confined in a two-dimensional space could be a first step towards the understanding of chiral interactions in more complex systems. But research is limited by the fact that pure enantiomers are not always available. Moreover energies due to chiral interactions are generally negligible in comparison with other attractive or repulsive sources. Expected effects can only be detected with very accurate apparatus. Thus, 2-alcohols are good candidates because on the one hand the pure enantiomer synthesis is known and on the other they form quite large crystals (close to the mm range) at the water surface which can be analysed now with the very high resolution provided by new generation synchrotron beamlines. For short 2-alcohols, the air/water interface does not induce chiral separation, a heterochiral behavior attraction is detected in two dimensions. The same results are observed in the 3D, racemic bulk crystals [13] being racemate. But at the water surface, the disorder of the rotator phase favored a solid solution instead of a racemate because the interface allows disorder which explains 2D/3D differences. Contrary to other crystalline monolayers (for example [25]), the hexagonal rotator phase structure is not affected by chirality, rather the enantiomeric excess of left molecules can be seen as impurities and consequently the melting of the 2D crystal is broader than for a pure one, explaining the decrease in monolayer rigidity observed for mixtures other than 50/50 or 100/0.

We would like to acknowledge Bruno Berge for his great help during all this research project, as well as for experiments and for many scientific discussions, and also Janine Lajzerowicz for fruitful discussions. This article is dedicated to the memory of Andrè Collet.

References

1. J. Jacques, A. Collet, S.H. Wilen, *Enantiomers, Racemates and Resolutions* (Wiley, New York, 1981).
2. E.J. Ariens, Trends Pharmacol. Sci. **14**, 68 (1993).
3. U. Hacksell, S. Ahlenius, Trends Biotechnol. **11**, 73 (1993).
4. E.M. Arnett, O. Thompson, J. Am. Chem. Soc. **103**, 968 (1981).
5. R.M. Weis, H.M. McConnell, J. Phys. Chem. **89**, 4453 (1985).
6. P. Nassoy, M. Goldmann, O. Bouloussa, F. Rondelez, Phys. Rev. Lett. **75**, 457 (1995).
7. E. Scalas, G. Brezesinsky, H. Möhwald, K.G. Kaganer, W.G. Bouwman, K. Kjaer, Thin Solid Films **284**, 56 (1996).
8. E. Scalas, G. Brezesinski, V.M. Kaganer, H. Möhwald, Phys. Rev. E **58**, 2172 (1998).
9. I. Kuzmenko, R. Buller, W.G. Bouwman, K. Kjaer, J. Als-Nielsen, M. Lahav, L. Leiserowitz, Science **274**, 2046 (1996).
10. D. Andelman, J. Am. Chem. Soc. **111**, 6536 (1989).
11. B. Berge, A. Renault, Europhys. Lett. **21**, 773 (1993).
12. B. Berge, O. Konovalov, J. Lajzerowicz, A. Renault, J.P. Rieu, M. Vallade, Phys. Rev. Lett. **73**, 1652 (1994).
13. A. Renault, C. Alonso, F. Artzner, B. Berge, M. Goldmann, C. Zakri, Euro. Phys. J. B **1**, 189 (1998).
14. A.A. Kandil, K.N. Slessor, Can. J. Chem. **61**, 1166 (1983).
15. A. Renault, O. Schultz, O. Konovalov, B. Berge, Thin Solid Films **248**, 47 (1994).
16. R.M.A. Azzam, N.M. Bashara, *Ellipsometry and Polarized Light* (North Holland Personal Library, Amsterdam, 1977).
17. *HERCULES, Theory, Instruments and Methods*, Vol. **1** (Les Editions de Physique - Springer Verlag, 1994).
18. C. Zakri, A. Renault, J.P. Rieu, M. Vallade, B. Berge, J.F. Legrand, G. Vignault, G. Grübel, Phys. Rev. B **55**, 163 (1997).
19. J.P. Rieu, PhD Thesis, Université Joseph Fourier-Grenoble I, 1995.
20. D.R. Nelson, B.I. Halperin, Phys. Rev. B **19**, 2457 (1979).
21. C. Alonso, PhD Thesis, Université Joseph Fourier-Grenoble I, 1999.
22. J.W. Christian, *The Theory of Transformations in Metals and Alloys*, Vol. **7** (Pergamon Press, Oxford, 1965).
23. J. Lajzerowicz, J. Lajzerowicz-Bonneteau, B. Suchod, J. Phys. I **1**, 573 (1991).
24. R. Zantl, L. Baicu, F. Artzner, I. Sprenger, G. Rapp, J.O. Rädler, J. Phys. Chem. B **103**, 10300 (1999).
25. C. Böhm, H. Möhwald, L. Leiserowitz, J. Als-Nielsen, K. Kjaer, Biophys. J. **64**, 553 (1993).